Bioresource Technology 318 (2020) 124104

Contents lists available at ScienceDirect

Bioresource Technology

journal homepage: www.elsevier.com/locate/biortech

Production and high throughput quantification of fucoxanthin and lipids in *Tisochrysis lutea* using single-cell fluorescence

Fengzheng Gao[a,*], Iago Teles (Cabanelas, ITD)[a], Narcís Ferrer-Ledo[a], René H. Wijffels[a,b], Maria J. Barbosa[a]

[a] Wageningen University, Bioprocess Engineering, AlgaePARC, P.O. Box 16, 6700 AA Wageningen, Netherlands
[b] Faculty Biosciences and Aquaculture, Nord University, N-8049 Bodø, Norway

GRAPHICAL ABSTRACT

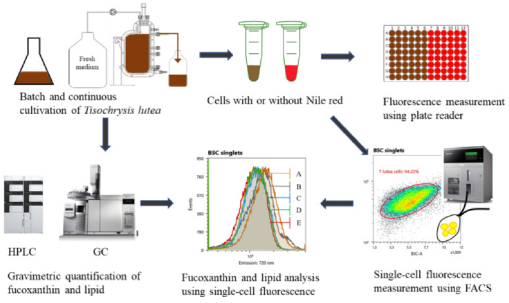

ARTICLE INFO

Keywords:
Fucoxanthin
Single-cell
Fluorescence-activated cell sorting (FACS)
Polar/neutral lipids
Chlorophyll

ABSTRACT

This work aimed to investigate the accumulation of fucoxanthin and lipids in *Tisochrysis lutea* during growth (N+) and nitrogen-starvation (N−) and to correlate these products with single-cell emissions using fluorescence-activated cell sorting (FACS). Fucoxanthin content decreased 52.94% from N+ to N− in batch cultivation; increased 40.53% as dilution rate changed from 0.16 to 0.55 d^{-1} in continuous cultivation. Total lipids (N−) were constant (~250 mg/g), but the abundance of neutral lipids increased from 4.87% to 40.63%. Nile red can stain both polar and neutral lipids. However, in vivo, this differentiation is limited due to an overlapping of signals between 600 and 660 nm, caused by neutral lipids concentrations above 3.48% (W/W). Chlorophyll autofluorescence (720 nm) was reported for the first time as a proxy for fucoxanthin (R^2 = 0.90) and polar lipids (R^2 = 0.98). FACS can be used in high throughput quantification of pigments and lipids and to select and sort cells with high-fucoxanthin/lipids.

1. Introduction

In the past years, *Tisochrysis lutea* (*T. lutea*) has obtained increased interests for fucoxanthin (Fx) and lipid production. Fx is of interest due to its biological properties, such as antioxidant, anti-obesity, and anti-diabetic (Fung et al., 2013; Maeda et al., 2018). *T. lutea* contains up to 18.23 mg/g dry weight (DW) Fx and 32% of total fatty acids DW (Balduyck et al., 2016; Kim et al., 2012). The fatty acids are typically classed as polar or neutral lipids. Polar lipids are the main structural fatty acids that can be utilized as functional additive in food or feed, while neutral lipids serve as storage lipids that can be used for biofuels (Mairet et al., 2011). Within the lipids in *T. lutea*, the long-chain omega-

* Corresponding author.
E-mail address: fengzheng.gao@wur.nl (F. Gao).

https://doi.org/10.1016/j.biortech.2020.124104
Received 20 August 2020; Received in revised form 31 August 2020; Accepted 3 September 2020
Available online 10 September 2020

3 fatty acid docosahexaenoic acid (DHA), is associated with numerous health benefits such as promoting fetal development, including neuronal, retinal, and immune function, improving cardiovascular function such as inflammation, peripheral artery disease (Swanson et al., 2012). In addition to health benefits for humans, Fx and long-chain omega-3 fatty acids also play a key role in health and development of aquatic organisms, which makes *T. lutea* a widely used feed in aquaculture (Bigagli et al., 2018).

Fx and polar/neutral lipids quantification are essential to assess the quality of *T. lutea* biomass. The traditional methods for pigment and polar/neutral lipids measurements are high-performance liquid chromatography (HPLC) and gas chromatography (GC) respectively (Foo et al., 2017; He et al., 2019; Niemi et al., 2019). These techniques are common methods for the detection of these compounds with acceptable accuracy. However, complex pre-treatments such as freeze drying and cell disruption are required for both methods; several organic chemicals, such as chloroform, methanol, and hexane, are used in the extraction procedure, which are not environmentally-friendly. In addition, a relatively large amount of biomass needs to be used to meet the limit of detection, which limits the number of samples which can be taken. Hence, HPLC and GC are expensive, as well as time and biomass consuming. A rapid method was developed for the determination of Fx in Diatom using spectrophotometry (Li et al., 2018). However, ethanol extraction was still needed for this method. Therefore, a fast method using high-throughput techniques is needed for process control and strain selection.

A promising alternative technique based on FACS offers high throughput and fast analysis of microalgal cells (Park et al., 2019; Pereira et al., 2018). It is a fast, reliable and efficient method that can detect the compounds based on the fluorescence signal from single cells and can also be used for metabolic monitoring (Li and Wilkins, 2020). Previous research studied the possibilities to use FACS for high lipid content microalgal cells selections with Nile red (NR) or BODIPY for neutral lipids staining (Cabanelas et al., 2016; Chen et al., 2009). Monitoring and screening high-polar lipids cells are getting more attention due to more functional applications. However, the ability of FACS to distinguish the fluorescence signals from polar and neutral lipids in *T. lutea* is still missing. Concerning Fx, no previous studies have reported the use of FACS for determination of this compound. Therefore, the use of FACS to measure polar lipids and fucoxanthin was explored. Moreover, correlations between concentrations of these compounds could make it possible to detect them in simultaneously.

This study aimed to develop a method for high throughput measurement of Fx, polar and neutral lipids in *T. lutea* using FACS. To do so, correlations were analysed between these compounds with single-cell fluorescence. Batch and continuous experiments were designed to produce *T. lutea* with varying concentrations of pigments and lipids by varying light and nitrogen concentration. Plate reader and FACS were used to analyse the autofluorescence of pigments and the fluorescence of lipids stained with NR. This study established reliable correlations between single-cell fluorescence and cellular contents of Fx, polar/neutral lipids, and chlorophyll *a* (chl-a) consequentially, allowing the use of FACS as a high-throughput tool to monitor these compounds in *T. Lutea*.

2. Methods and materials

2.1. Microalgal strain and cultivation medium

Tisochrysis lutea (previously named as *Isochrysis galbana* (Bendif et al., 2013)) and commercial culture medium NutriBloom plus (Fernandes et al., 2016) were obtained from NECTON, S.A. (Olhão, Portugal). Mineral composition of NutriBloom plus: $NaNO_3$ 2 M, KH_2PO_4 100 mM, $ZnCl_2$ 1 mM, $ZnSO_4$ 1 mM, MnCl 1 mM, Na_2MoO_4 0.1 mM, CoCl 0.1 mM, $CuSO_4$ 0.1 mM, EDTA 26.4 mM, $MgSO_4$ 2 mM, $FeCl_3$ 20 mM, Tiamina 35 mM, Biotina 5 mg/L, vitamin B_{12} 3 mg/L. The cultivation medium was prepared with natural seawater from the North Sea (The Netherlands) enriched with 2 mL/L of the NutriBloom plus stock with 4 mM final nitrogen ($NaNO_3$) concentration and a pH = 8.0 (containing 20 mM HEPES).

2.2. Batch experiment

T. lutea was cultivated in 250 mL flasks containing 100 mL medium at 25 °C, light intensity 140 μmol m^{-2} s^{-1}, 150 rpm and 2% CO_2. A 18:6 day:night photoperiod was applied for cultivation under photoautotrophic conditions. All flasks had the same initial biomass concentration with a 0.2 optical density (OD) at 750 nm. The flasks were changed positions in incubators randomly every day to avoid the effect of different light intensities at different positions. A volume of 200 mL culture was harvested every day for Fx and lipid measurement. The batch experiment lasted for 8 days.

2.3. Continuous chemostat experiments

T. lutea was inoculated into flat-panel photobioreactors (Algaemist (Breuer et al., 2012), light path 14 mm) containing 400 mL NutriBloom medium at a light intensity of 300 μmol m^{-2} s^{-1} with an 18:6 day:-night cycle and at 30 °C. The cultures were diluted at different specific dilution rates: 0.16, 0.28, 0.35, 0.51, 0.55 d^{-1} (chemostat experiments (Gao et al., 2020)). The overflow culture from the Algaemist was harvested every day for Fx and lipid analysis.

2.4. Daily measurements

The OD_{750} of cultures was measured with a 1.0 cm light path cuvette in a HACH LANGE DR600 spectrophotometer. Cell number and size were measured using a Beckman Coulter Multisizer. To measure the dry weight (DW), 2 mL of culture was diluted with 50 mL 0.5 M ammonium formate and filtered through a pre-dried Whatman GF/F filter (0.7 μm pore size) and washed twice with 50 mL ammonium formate. Cells on the filters were dried at 100 °C in the oven for 24 h (until constant weight) and were subsequently cooled to room temperature in a desiccator for 2 h before weighting. The maximal photosystem II quantum yield (QY) was measured using an AquaPen AP100 after culture dark adaptation for 10 min to determine the ratio of variable fluorescence to maximal fluorescence (Parkhill et al., 2001). The overflow volume in chemostat experiments were measured every day. The harvested culture from batch and continuous experiments was centrifuged in 50 mL Greiner falcon tubes at 4255 × *g* for 5 min. After discarding the supernatant, the cell pellets were resuspended and combined in 50 mL 0.5 M ammonium formate and were centrifuged using the same centrifugation settings. The washing step with ammonium formate was repeated twice. The cell pellets after washing were flushed with N_2 and stored in a freezer at approximately −20 °C. The nitrate in medium was checked using MQuant™ Nitrate Test (Merck KGaA, Germany). To obtain the supernatant, 2 mL culture was centrifuged at 10000 × *g* for 2 min. The test strip was immersed in the supernatant for 1 s and the excess liquid was shaken off. The nitrate was determined with the colour on the label after 1 min reaction.

2.5. Pigments extraction and measurement

The frozen harvest biomass was freeze dried (Sublimator 2 × 3 × 3 5, Zirbus Technology, the Netherlands) for 41 h. Small samples of biomass (1–2 mg) were extracted with 1 mL of ethanol using bead beater tubes (MP Biomedicals, REF 6914–500, composition: 1.4 mm ceramic spheres, 0.1 mm silica spheres, and one 4 mm glass sphere) in a beater (Bertin Technologies). Fx extraction and sample preparation were performed according to the previous reported methods (Gao et al., 2020). To quantify the concentration of Fx and chl-a, samples were run in a HPLC (Shimadzu, Nexera UHPLC) according to Grant (2011). The

injected sample volume was 20 μL, the stationary phase was a C18 column (Kinetex C18 5 μm 100 Å 150 × 4.6 mm). The standards of Fx and chl-a were from Sigma-Aldrich and were diluted with methanol to different concentration of 0, 2, 4, 6, 8, 10 μg/mL for concentration calibration.

2.6. Fatty acids extraction and measurement

Fatty acids extraction, separation into polar and neutral lipids and quantification were performed as described by Remmers et al. (2017). Approximately 10 mg of freeze-dried biomass was weighted for lipid extraction. Chloroform: methanol (v:v = 2:2.5) solution with added internal standard (pentadecanoic acid (neutral lipid) and decanoic acid (polar lipid)) was used as extraction solvent. After extraction, polar and neutral lipids were separated using an SPE column (Sep Pak Vac Silica cartridge, 6 cc, 1000 mg, Waters). The columns were equilibrated with 10 mL hexane. Concentrated samples were resuspended in 1.5 mL hexane/diethylether (v:v = 7:1) and loaded onto the column. Then, neutral lipids were eluted using 10 mL of hexane/diethylether (v:v = 7:1), which was collected in a fresh glass tube. Subsequently, polar lipids were eluted with 10 mL methanol/acetone/hexane (v:v:v = 2:2:1) and collected in fresh glass tubes. Samples were evaporated with N_2 at 30 °C.

To detect fatty acids with GC, the fatty acids were methylated. To every sample, 3 mL of methanol/sulfuric acid (v:v = 95:5) was added, after which the samples were heated at 70 °C for 3 h. After cooling to room temperature, 3 mL water and 3 mL hexane was added to the samples. The samples were mixed for 15 min and centrifuged for 5 min (1204 × *g*, 15 °C). 2 mL of the hexane phase was transferred to fresh glass tubes, which was then washed with 2 mL water. The hexane phase was used for GC analysis.

An Agilent 7890 GC system (Santa Clara, CA, USA) was used to determine the lipid contents. GC vials were filled with the sample containing hexane phase and placed in the autosampler. A Supelco Nucol 25357 column (30 m × 530 μm × 1.0 μm) was used with hexane as running solvent and helium as carrier gas (20 mL min^{-1}). Data was collected and processed with Openlab software (7890 GC). The total fatty acids was calculated by summing polar and neutral lipids.

2.7. Fluorescence measurement

2.7.1. Fluorescence measurement in batch using plate reader

The culture was diluted to OD_{750} = 0.2 using fresh medium and an amount of 100 μL was pipetted in triplicate in a black 96-well plate with transparent cover to avoid signal interference from different wells. The cells were stained with NR (final concentration 2 μg/mL) for 5 min in dark (Bertozzini et al., 2011; Sakurai et al., 2016). The NR fluorescence was measured from the top using a Synergy HTX Multi-Mode Microplate Reader at an excitation wavelength of 488 nm with an emission wavelength range from 530 nm to 800 nm. The NR fluorescence was measured every day at the same time for each batch experiment. The autofluorescence was measured using the same procedure without NR staining.

2.7.2. Single-cell fluorescence measurement using FACS in continuous experiment

Samples were collected every day (approximately 1 h before the dark period started) from the Algaemist and were diluted to OD_{750} = 0.2 using fresh medium. To measure the autofluorescence of the single cells, 200 μL sample was analysed by FACS (Sony Cell Sorter SH800S) with 100 μm microfluidics sorting chip (LE-C3210, Sony, Japan). A 488 nm laser was used to excite compounds, three emission channels (FL2 585/30, FL3 617/30, FL5 720/60) were applied for the fluorescence detection. Cells for fluorescence measurement were selected from three different density plots. Firstly, the backward scatter area (BSC-A) was plotted against the forward scattered light area (FSC-A) to distinguish bacteria and other impurities from the microalgae. A gate was created to select only microalgal cells. Next, the FSC corresponding to a cells' height was plotted against the FSC area to select single-cells. Finally, a gate was created in a BSC height versus area plot to include all cells. The fluorescence signal was recorded for two minutes.

The fluorescence associated to lipids was measured following the staining method reported in the batch section. The NR fluorescence was measured as the method described for autofluorescence. The survival rate of the single cells was analysed after the sorting procedure. Single cells with or without NR staining were sorted to 96-well plate with 100 μL medium in each well. Each well has one single-cell. The cells were incubated in a climate room at light intensity ~ 40 μmol m^{-2} s^{-1}, 25 °C. The wells with growing cells were counted after 7–10 days incubation.

2.8. Statistical analyses

The results were analysed based on the data from at least three different points during steady state in continuous experiments. Single-cell fluorescence signals were obtained from 100 000 events. Experimental results were expressed as mean value ± SD. Differences between groups were tested for significance by the least significant difference mean comparison using the IBM® SPSS® Statistics software (version 25) software program. The relationship between variables was determined by one-way ANOVA at a significance level of 0.05 using a Duncan Post-Hoc test.

3. Results and discussion

3.1. Content and fluorescence of pigments and polar/neutral lipids in batch cultivation

3.1.1. Fucoxanthin and chlorophyll dynamics during growth

During batch cultivation, the fucoxanthin (Fx) content increased rapidly in the first three days of exponential growth, from 6.83 mg/g to 13.09 mg/g, and then declined 52.94% to 6.16 mg/g (Fig. 1a). This decline is due to nitrogen starvation which started at the middle of day 3, when all nitrogen was consumed, and lasted until the end of the experiment (day 8). Chl-a followed a similar trend as Fx, showing an increase from 8.20 mg/g to 18.94 mg/g from day 1 to day 3 and a decrease to 4.87 mg/g at day 8 (Fig. 1b). The Fx and chl-a contents in *T. lutea* showed a high positive correlation (Fig. 1b; R^2 = 0.95). In microalgal cells, Fx is bound to protein complexes forming the Fx-chlorophyll protein (FCP), which can be found inside the thylakoid membrane (Pyszniak and Gibbs, 1992). The crystal structure of FCP reported in *Phaeodactylum tricornutum* reveals the binding of seven chl-a, two chl-c and seven Fx (Wang et al., 2019). Fx is the major light harvesting pigment surrounded by chlorophyll, enabling the energy transfer and quenching via Fx with high efficiency.

Nitrogen plays a key role in pigment accumulation. Similar to our results, the Fx content in *P. tricornutum* was higher with 14.5 mM nitrogen (6.56 mg/g) than that with 2.9 mM nitrogen (5.53 mg/g) after 12 days cultivation (Gao et al., 2017). Fx is a primary pigment in *Isochrysis* (Custódio et al., 2014) and, like chlorophyll, is correlated with cellular replication (i.e., formation of new biomass). In the present study, the initial nitrogen concentration was planned to be low (4 mM) and consumed at day 3, which was confirmed by non-detectable concentrations of nitrogen. After that, photosynthesis continues but no new functional (nitrogen-rich) biomass can be produced, which resulted in the declined fucoxanthin content.

3.1.2. Total, polar, and neutral lipids dynamics in batch cultivation

The nitrogen (4 mM $NaNO_3$) in the medium was sufficient for three days cultivation. *T. lutea* was cultivated at nitrogen starvation (no nitrogen) condition from day 4 to 8. The total fatty acids (TFA) content

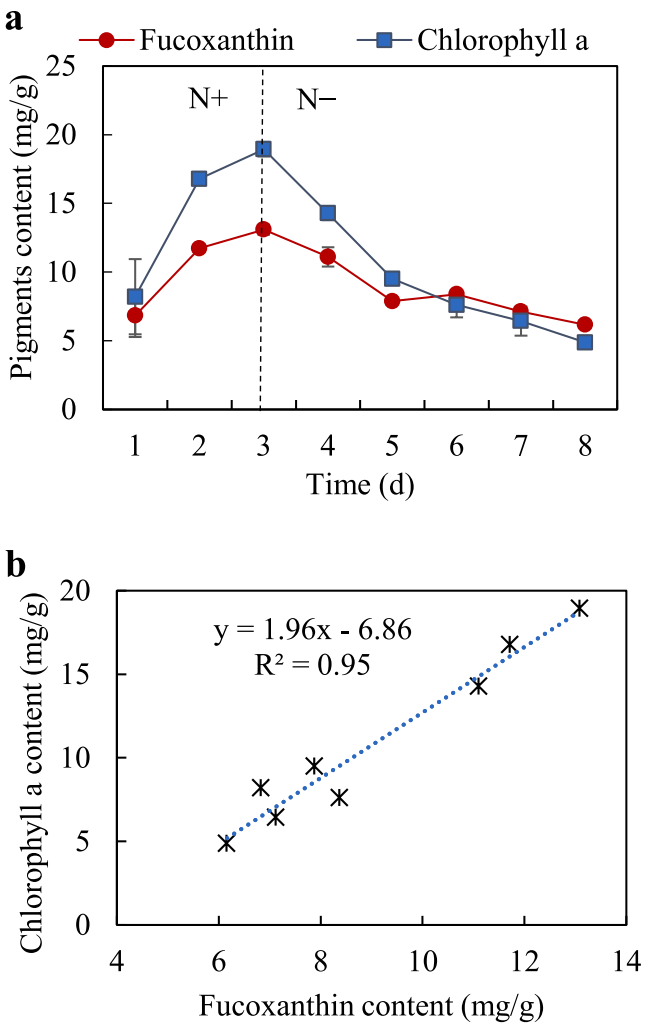

Fig. 1. Pigments contents (a) and correlation between fucoxanthin and chlorophyll *a* contents (b) of *Tisochrysis lutea* in batch. Note: Nitrogen-starvation started at day 3; values are the means ± SD.

remained constant (approximately 250 mg/g) during nitrogen starvation, and were higher than during nitrogen-sufficient period (164.60–200.98 mg/g) (day 1–3) (Fig. 2a). The polar lipids were the main lipid fraction in the first three days (208.39 mg/g) but decreased to 137.41 mg/g from day 4 to day 8 (Fig. 2a). On the contrary, the neutral lipid content increased from 6.81 mg/g to 94.02 mg/g from day 3 to day 8 (Fig. 2a). The percentage of polar lipids in TFA decreased from 95.13% to 59.37%, while the percentage of neutral lipids increased from 4.87% to 40.63% of TFA, under nitrogen starvation.

Neutral lipids are accumulated during nitrogen depletion (Benvenuti et al., 2016), which explained their increase after day 3 (Fig. 2a). It is hypothesized that the polar lipids were converted to neutral lipids while TFA stayed constant from day 4 to day 8. A conversion of membrane lipids to storage lipids was observed after changing nitrogen availability in *T. lutea* (Garnier et al., 2016). In addition, the cellular triacylglycerol (proportion in neutral lipids) content (pg cell^{-1}) in *T. lutea* increased significantly from logarithmic (166–240 fg cell^{-1}) to stationary phase (539–566 fg cell^{-1}) (da Costa et al., 2017). Moreover, neutral lipids accumulation was reported under nitrogen limitation conditions in *T. lutea* due to inducing a reorganization of thylakoid membranes (Huang et al., 2019).

3.1.3. Correlation between polar/neutral lipids content and Nile red fluorescence

The fluorescence of NR-stained cells showed emission signals within

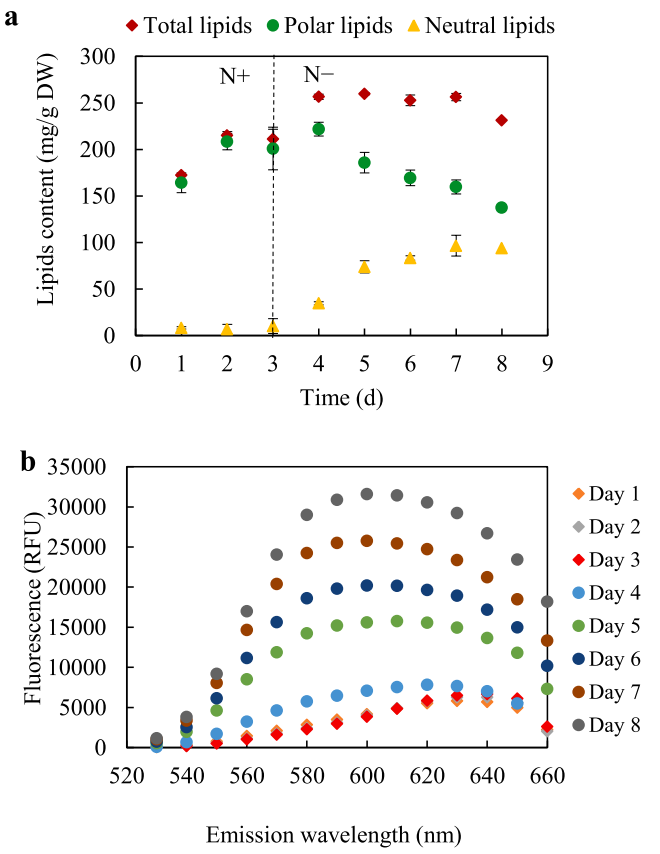

Fig. 2. Total, polar, and neutral lipids dynamics (a) and Nile red fluorescence (b) of *Tisochrysis lutea* grown in batch mode. Note: N-starvation started at day 3; values are the means ± SD. (For interpretation of the references to colour in this figure legend, the reader is referred to the web version of this article.)

the range of 540–660 nm (Fig. 2b). The fluorescence peak was at 620–640 nm for the first three days when the major lipids were 95% polar (Fig. 2b). However, the fluorescence peak shifted to 590–610 nm when the amount of neutral lipids was above 3.48% (W/W) (Fig. 2a, b). This means that with NR staining, polar and neutral lipids can be distinguished from each other. However, only if cells have < 3.48% (W/W) neutral lipids, the detected fluorescence can be associated with polar lipids. This limitation is explained by the fact that the fluorescence peaks of polar and neutral lipids are close to each other. Therefore, they are difficult to be differentiated. Similar results were found by Alonzo and Mayzaud (1999) using polar and neutral lipid standards. The NR staining fluorescence emission spectrum of phosphatidylcholine (polar lipid standard) ranged from 530 to 680 nm with a peak at 610 nm with excitation at 530 nm. However, the emission spectrum of triolein (neutral lipid standard) shifted 30 nm towards lower wavelengths ranging from 520 to 660 nm with a peak at 580 nm. (Alonzo and Mayzaud, 1999) The overlay between polar and neutral lipids was also observed. Similar results were obtained in vivo for the first time, as found using standards.

The ratio of polar/neutral lipids changes depending on the cultivation stage or metabolic activity of the cells. Consequentially, it is possible to monitor the fluorescence signals associated with these lipid classes as a proxy for gravimetric methods. Thus, fluorescence from 620 and 590 nm can be used for polar and neutral lipids detection in *T. lutea*. Therefore, the ratio of polar/neutral lipids was positively correlated with the ratio 620/590 nm (R^2 = 0.99), allowing us to estimate the relative lipid composition by assessing single-cell lipid fluorescence. Similar correlations were observed between the cellular contents in polar and neutral lipids and the signal of microalgal cells marked with NR (575 nm signal-neutral lipids, R^2 = 0.87; 620 nm signal-polar

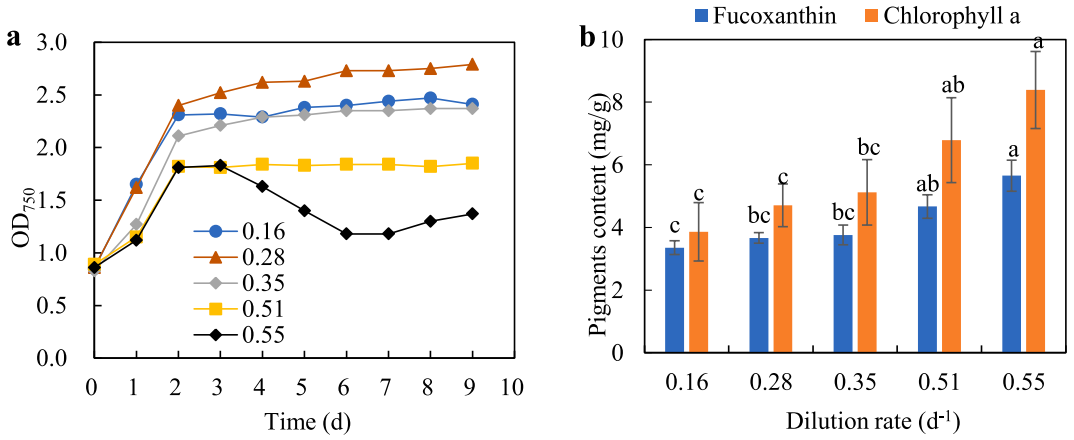

Fig. 3. Growth (a) and pigments content of *Tisochrysis lutea* in continuous chemostat experiments. Note: values are the means ± SD; Bars with different letters are significantly different from each other ($p < 0.05$).

lipids, $R^2 = 0.61$) (Guzmán et al., 2011; 2010). NR staining is a common method to detect neutral lipids in microalgal cells. For instance, Bertozzini et al. (2011) reported the NR method (excitation wavelength 547 nm; emission wavelength 580 nm) for the absolute quantification of neutral lipids in *Skeletonema marinoi*, *Chaetoceros socialis,* and *Alexandrium minutum*. In the present study, the emission fluorescence signals at 620 nm and 590 nm (excited at 488 nm) can be used for polar and neutral lipids detection.

3.2. Content and fluorescence of pigments and lipids in continuous cultivation

3.2.1. Growth, fucoxanthin and chlorophyll contents in chemostat experiments

Several chemostat experiments were performed at different dilution rates of 0.16, 0.28, 0.35, 0.51 and 0.55 d^{-1} with a limiting nitrogen concentration (Fig. 3a). The nitrogen was supplied by dropping from the fresh medium vessel, which was consumed by *T. lutea* immediately. Therefore, no nitrogen (NO_3^-) can be detected from the culture. Nitrogen supplementation was higher at higher dilution rates. The biomass concentration was higher at lower dilution rates, with the exception at 0.28 d^{-1}, which was higher than the biomass at 0.16 d^{-1} (Table 1).

The chl-a content was positively correlated to Fx content ($R^2 = 0.99$) and in line with the results obtained in batch ($R^2 = 0.95$). The Fx content increased 40.53% from 3.36 mg/g to 5.65 mg/g ($p < 0.05$) and the chl-a content increased from 3.86 to 8.39 mg/g as the dilution rate increased from 0.16 d^{-1} to 0.55 d^{-1} (Fig. 3b). Since the nitrogen supply rate is a function of the dilution rate (i.e., growth), so was chl-a content a function of nitrogen supply rate (Fig. 3b). The reduction in *Isochsysis galbana* pigmentation was reported before under nitrogen limitation (Falkowski et al., 1989). With decreasing dilution rate from 0.96 to 0.18 d^{-1} in nitrogen limited chemostat mode, the cellular chl-a decreased 50% in that study (Falkowski et al., 1989).

3.2.2. Correlation between pigment and lipid content

A positive correlation ($R^2 = 0.88$) was found between Fx content and chl-a content when combining data from chemostat experiments with those from batch experiment (Fig. 4). This correlation is valid at different cultivation settings with different Fx and chl-a concentrations.

The TFA content ranged from 25.59% to 31.43% DW without obvious trends (Table 1). The percentage of polar lipids of TFA increased from 36.98% to 54.78% and the content increased from 116.28 to 157.49 mg/g as increasing dilution rate from 0.16 to 0.55 d^{-1} (Table 1). In continuous cultivation, the maximum percentage of polar lipids in TFA (54.78%) was lower than the minimum percentage (59.37%) measured in batch, which indicates that a continuous nitrogen limitation leads to a further decrease of the polar lipids. Moreover, the TFA content in continuous nitrogen limited conditions was higher than in batch, reaching 31.34%. The stable TFA content was reported during starvation period in batch. The higher TFA in continuous chemostat experiments was probably related to the different cultivation parameters such as light intensity and temperature.

The correlations between pigment and lipid were analysed both for batch and continuous experiments. Fx content was positively correlated to chl-a content (Fig. 4; $R^2 = 0.88$) and polar lipids (Fig. 4; $R^2 = 0.88$). Polar lipids are described as membrane-bound while Fx and chl-a are combined in FCP in membrane. Hence, these compounds are all membrane-bound, which explains the positive correlations. To our knowledge, this is the first study reporting the correlations between these three compounds in *T. lutea*, which is a useful evidence for detecting these compounds simultaneously.

Table 1
Growth and compounds details in chemostat experiments at different dilution rates.

Dilution rate (d^{-1})	0.16	0.28	0.35	0.51	0.55
$NaNO_3$ (mg/d)	21.76	30.08	47.59	69.35	74.79
μ (d^{-1})	0.16 ± 0.01^{e}	0.28 ± 0.01^{d}	0.35 ± 0.02^{c}	0.51 ± 0.02^{b}	0.55 ± 0.03^{a}
QY (Fv/Fm)	0.64 ± 0.008^{c}	0.68 ± 0.006^{b}	0.71 ± 0.003^{ab}	0.74 ± 0.003^{a}	0.73 ± 0.006^{a}
Cell number (10^7/mL)	2.95 ± 0.05^{b}	3.83 ± 0.13^{a}	2.79 ± 0.06^{c}	2.52 ± 0.09^{d}	1.61 ± 0.15^{e}
Diameter (μm)	6.14 ± 0.06^{a}	5.75 ± 0.09^{b}	6.23 ± 0.10^{a}	6.18 ± 0.08^{a}	6.21 ± 0.10^{a}
Biomass concentration DW (g/L)	1.11 ± 0.02^{b}	1.26 ± 0.07^{a}	0.97 ± 0.04^{c}	0.68 ± 0.02^{d}	0.39 ± 0.01^{e}
ΣFA%/DW	31.43 ± 0.97^{a}	25.59 ± 0.36^{b}	26.73 ± 0.89^{ab}	30.33 ± 2.24^{ab}	28.8 ± 2.45^{ab}
Σpolar/ΣFA	36.98 ± 1.71^{c}	46.09 ± 1.95^{b}	43.25 ± 2.40^{b}	46.97 ± 1.40^{b}	54.78 ± 2.24^{a}
Polar lipids content (mg/g)	116.28 ± 6.79^{b}	117.88 ± 4.95^{b}	115.31 ± 5.98^{b}	142.56 ± 11.83^{ab}	157.49 ± 14.02^{a}
Fx cell content (pg/cell)	0.123 ± 0.016	0.122 ± 0.008	0.133 ± 0.022	0.128 ± 0.021	0.148 ± 0.026

Note: values are the means ± SD. Means with different letters are significantly different ($p < 0.05$).

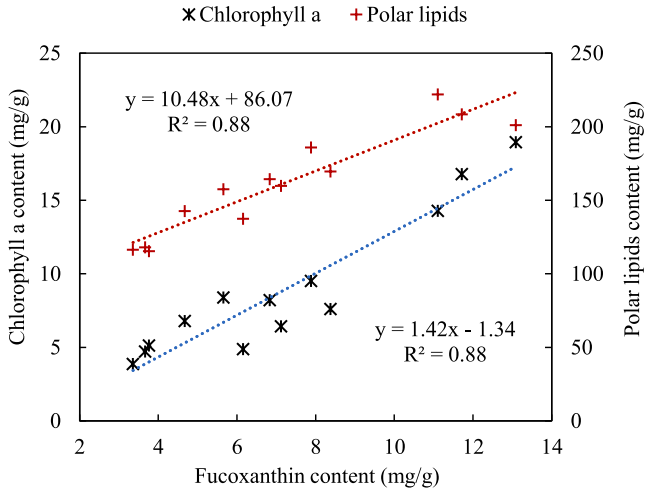

Fig. 4. Correlation between fucoxanthin and chlorophyll *a* and correlation between fucoxanthin and polar lipids. Note: data collected from both batch and continuous experiments.

3.2.3. Correlation between intracellular fucoxanthin or polar/neutral lipids content and single-cell fluorescence

The autofluorescence spectrum showed the distributions of the fluorescence signal from single cells (Fig. 5). The mean intracellular Fx content increased from 0.122 to 0.148 pg/cell, corresponding to the increasing emission autofluorescence signal at 720 nm from FACS (Fig. 5). Intracellular Fx content was positively correlated to single-cell fluorescence (R^2 = 0.90). Therefore, single-cell fluorescence at 720 nm can be used for Fx measurement. The emission bands of extracted Fx from brown algae were around 630, 685 and 750 nm (Katoh et al., 1991). Although the emission brands of extracted Fx can be detected, these bands cannot be distinguished from intracellular Fx due to overlapped signals from multi-compounds and energy transfer from Fx to chlorophyll inside FCP. The emission fluorescence of isolated FCP from diatoms involved in non-photochemical quenching ranged from

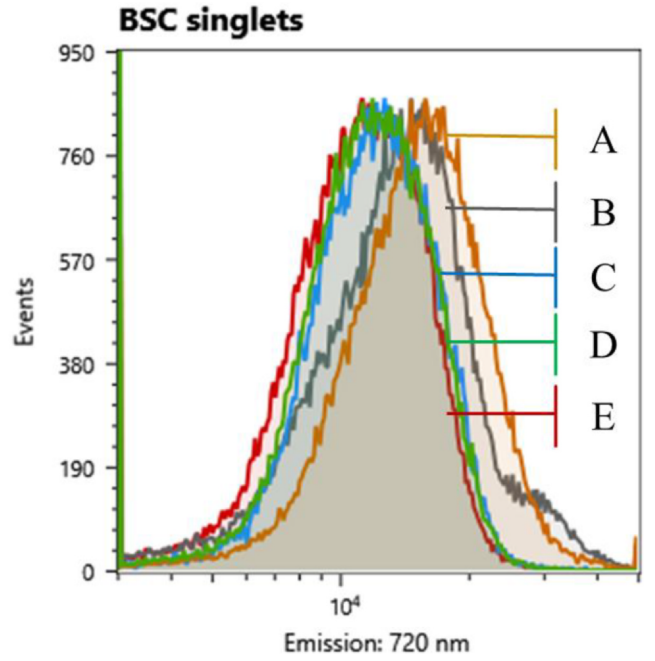

Fig. 5. Single-cell fluorescence emission signals at 720 nm of *Tisochrysis lutea* in continuous chemostat experiments. Note: Excited wavelength of all experiments is 488 nm. Letters in the figure corresponding to fucoxanthin cell content (pg/cell): A: 0.148; B: 0.133; C:0.128; D:0.123; E:0.122.

680 to 725 nm (Gundermann and Büchel, 2012; Miloslavina et al., 2009). The single-cell fluorescence found at 720 nm in the present study was probably excited from FCP in *T. lutea* as well. However, the structure and working mechanism of FCP may differ with microalgal species.

The ratio (0.59–1.21) of polar/neutral lipids was positively related to the ratio (1.13–1.52) of single-cell fluorescence at 617 nm/585 nm from FACS (R^2 = 0.89); similar to the results in batch using a plate reader. In addition, intracellular polar lipids content was positively correlated to chl-a autofluorescence (R^2 = 0.98). Similar relationships between lipid and NR fluorescence was found in *Crypthecodinium cohnii* (De La Jara et al., 2003). The fluorescence signal ratio of FL3/FL2 (FL3 > 650 nm; FL2 560–640 nm) was linearly correlated with the neutral and polar lipid content (R^2 = 0.96). Although the emission lasers they used were different in this study, the relationships were similar. FACS showed a strong ability to analyse pigment and lipid contents by measuring single-cell fluorescence.

In the present study, the positive correlation between Fx and chl-a autofluorescence was found in both plate reader measurements from batch experiment and FACS measurements from continuous chemostat experiments. The relative neutral and polar lipids contents can be determined by NR fluorescence signal at 585 nm and 617 nm using FACS. Although many previous studies reported the ability of FACS for neutral lipid measurement (Cabanelas et al., 2015; De La Jara et al., 2003), this is the first work reporting Fx measurement using FACS.

3.3. Single-cell sorting and viability assay

In recent years, FACS has been widely used for high throughput measurement and cell selection (Hyka et al., 2013; Montero et al., 2011). The direct sorting onto solid medium upon FACS could save about 3 weeks during the scale-up process as compared to the growth of the same cultures in liquid medium (Pereira et al., 2011). The ability of FACS for high throughput measurement of pigments and lipids can be also used for the selection of high-Fx or high-lipids cells of *T. lutea*. Several previous studies reported protocols for viable microalgal cell sorting after staining with BODIPY or NR (Cabanelas et al., 2016, 2015; Montero et al., 2011; Yen Doan and Obbard, 2011). Nevertheless, some strains have been reported to be sensitive to the stress of the selection procedure (Elliott et al., 2012; Lee et al., 2013; Li et al., 2019). Therefore, the suitability of our method was evaluated in staining and sorting viable cells of *T. lutea*.

Using FACS as a selection tool in *T. lutea* strain improvement processes depends on cell survival after sorting. *T. lutea* is a sensitive microalgal species without cell wall. The single-cell viability of *T. lutea* was analysed after sorting with or without NR staining. Surprisingly, 77.5% single-cells sorted from the gate of autofluorescence at 720 nm survived while 80.0% single cells selected from the gate of NR staining fluorescence at 585 nm survived after sorting. Most of the cells can survive after sorting (Cabanelas et al., 2015). In this work, survival rates of 77.5% and 80.0% were observed for respectively non-stained and stained cells. This finding demonstrated FACS could be a promising tool in monitoring Fx and polar/neutral lipids and cell sorting of *T. lutea*. Cells with high autofluorescence at 720 nm are expected to have high Fx, chl-a and polar lipids contents.

The correlations between pigments and lipids make it possible to quantify these compounds in one single measurement. In the present study, it was shown that polar lipids can only be determined by NR fluorescence when its content is higher than 96.52% (W/W) of TFA. The positive correlations between these three compounds evidenced the use of autofluorescence from chl-a for both Fx and polar lipids determination. Compared to NR staining, autofluorescence without dye pre-treatment at 720 nm is more convenient for pigments and lipids monitoring and cell sorting due to the positive correlations between these compounds.

4. Conclusions

Here, batch and continuous experiments were conducted to produce biomass with varying concentrations of pigments and lipids. Fx was always coupled with chl-a and was positively correlated to polar lipids. Fx can be estimated by measuring chl-a autofluorescence emission at 720 nm. The polar/neutral lipids ratio can be monitored by NR fluorescence at 617 nm and 585 nm. High throughput measurement of pigments and polar/neutral lipids content in *T. lutea* were shown from single-cell fluorescence. FACS technique can be used in high throughput measurement of pigments and lipids and can be further applied in high-Fx/lipids cell selection for strain improvement.

CRediT authorship contribution statement

Fengzheng Gao: Investigation, Methodology, Formal analysis, Data curation, Software, Visualization, Writing - original draft, Writing - review & editing. **Iago Teles (Cabanelas, ITD):** Project administration, Formal analysis, Methodology, Supervision, Writing - review & editing. **Narcís Ferrer-Ledo:** Methodology, Formal analysis, Software, Writing - review & editing. **René H. Wijffels:** Project administration, Supervision, Writing - review & editing. **Maria J. Barbosa:** Project administration, Formal analysis, Funding acquisition, Methodology, Supervision, Writing - review & editing.

Declaration of Competing Interest

The authors declare that they have no known competing financial interests or personal relationships that could have appeared to influence the work reported in this paper.

Acknowledgements

This research is part of the MAGNIFICENT project, funded by the Bio Based Industries Joint Undertaking under the European Union's Horizon 2020 research and innovation program (grant agreement No. 745754).

Appendix A. Supplementary data

Supplementary data to this article can be found online at https://doi.org/10.1016/j.biortech.2020.124104.

References

Alonzo, F., Mayzaud, P., 1999. Spectrofluorometric quantification of neutral and polar lipids in zooplankton using Nile red. Mar. Chem. 67, 289–301. https://doi.org/10.1016/S0304-4203(99)00075-4.

Balduyck, L., Bijttebier, S., Bruneel, C., Jacobs, G., Voorspoels, S., Van Durme, J., Muylaert, K., Foubert, I., 2016. Lipolysis in T-Isochrysis lutea during wet storage at different temperatures. Algal Res. 18, 281–287. https://doi.org/10.1016/j.algal.2016.07.003.

Bendif, E.M., Probert, I., Schroeder, D.C., de Vargas, C., 2013. On the description of Tisochrysis lutea gen. nov. sp. nov. and Isochrysis nuda sp. nov. in the Isochrysidales, and the transfer of Dicrateria to the Prymnesiales (Haptophyta). J. Appl. Phycol. https://doi.org/10.1007/s10811-013-0037-0.

Benvenuti, G., Lamers, P.P., Breuer, G., Bosma, R., Cerar, A., Wijffels, R.H., Barbosa, M.J., 2016. Microalgal TAG production strategies: Why batch beats repeated-batch. Biotechnol. Biofuels 9, 1–17. https://doi.org/10.1186/s13068-016-0475-4.

Bertozzini, E., Galluzzi, L., Penna, A., Magnani, M., 2011. Application of the standard addition method for the absolute quantification of neutral lipids in microalgae using Nile red. J. Microbiol. Meth. 87, 17–23. https://doi.org/10.1016/j.mimet.2011.06.018.

Bigagli, E., Cinci, L., Niccolai, A., Biondi, N., Rodolfi, L., D'Ottavio, M., D'Ambrosio, M., Lodovici, M., Tredici, M.R., Luceri, C., 2018. Preliminary data on the dietary safety, tolerability and effects on lipid metabolism of the marine microalga Tisochrysis lutea. Algal Res. 34, 244–249. https://doi.org/10.1016/j.algal.2018.08.008.

Breuer, G., Lamers, P.P., Martens, D.E., Draaisma, R.B., Wijffels, R.H., 2012. The impact of nitrogen starvation on the dynamics of triacylglycerol accumulation in nine microalgae strains. Bioresour. Technol. 124, 217–226. https://doi.org/10.1016/j.biortech.2012.08.003.

Cabanelas, I.T.D., van der Zwart, M., Kleinegris, D.M.M., Barbosa, M.J., Wijffels, R.H., 2015. Rapid method to screen and sort lipid accumulating microalgae. Bioresour. Technol. 184, 47–52. https://doi.org/10.1016/j.biortech.2014.10.057.

Cabanelas, I.T.D., Van Der Zwart, M., Kleinegris, D.M.M., Wijffels, R.H., Barbosa, M.J., 2016. Sorting cells of the microalga Chlorococcum littorale with increased triacylglycerol productivity. Biotechnol. Biofuels 9, 1–12. https://doi.org/10.1186/s13068-016-0595-x.

Chen, W., Zhang, C., Song, L., Sommerfeld, M., Hu, Q., 2009. A high throughput Nile red method for quantitative measurement of neutral lipids in microalgae. J. Microbiol. Methods 77, 41–47. https://doi.org/10.1016/j.mimet.2009.01.001.

Custódio, L., Soares, F., Pereira, H., Barreira, L., Vizetto-Duarte, C., Rodrigues, M.J., Rauter, A.P., Alberício, F., Varela, J., 2014. Fatty acid composition and biological activities of Isochrysis galbana T-ISO, Tetraselmis sp. and Scenedesmus sp.: Possible application in the pharmaceutical and functional food industries. J. Appl. Phycol. 26, 151–161. https://doi.org/10.1007/s10811-013-0098-0.

da Costa, F., Le Grand, F., Quéré, C., Bougaran, G., Cadoret, J.P., Robert, R., Soudant, P., 2017. Effects of growth phase and nitrogen limitation on biochemical composition of two strains of Tisochrysis lutea. Algal Res. 27, 177–189. https://doi.org/10.1016/j.algal.2017.09.003.

De La Jara, A., Mendoza, H., Martel, A., Molina, C., Nordström, L., De La Rosa, V., Díaz, R., 2003. Flow cytometric determination of lipid content in a marine dinoflagellate, Crypthecodinium cohnii. J. Appl. Phycol. 15, 433–438. https://doi.org/10.1023/A:1026007902078.

Elliott, L.G., Feehan, C., Laurens, L.M.L., Pienkos, P.T., Darzins, A., Posewitz, M.C., 2012. Establishment of a bioenergy-focused microalgal culture collection. Algal Res. 1, 102–113. https://doi.org/10.1016/j.algal.2012.05.002.

Falkowski, P.G., Sukenik, A., Herzig, R., 1989. Nitrogen limitation in isochrysis galbana (haptophyceae). ii. relative abundance of chloroplast proteins. J. Phycol. https://doi.org/10.1111/j.1529-8817.1989.tb00252.x.

Fernandes, T., Fernandes, I., Andrade, C.A.P., Cordeiro, N., 2016. Changes in fatty acid biosynthesis in marine microalgae as a response to medium nutrient availability. Algal Res. 18, 314–320. https://doi.org/10.1016/j.algal.2016.07.005.

Foo, S.C., Yusoff, F.M., Ismail, M., Basri, M., Yau, S.K., Khong, N.M.H., Chan, K.W., Ebrahimi, M., 2017. HPLC fucoxanthin profiles of a microalga, a macroalga and a pure fucoxanthin standard. Data Br. 10, 583–586. https://doi.org/10.1016/j.dib.2016.12.047.

Fung, A., Hamid, N., Lu, J., 2013. Fucoxanthin content and antioxidant properties of Undaria pinnatifida. Food Chem. https://doi.org/10.1016/j.foodchem.2012.09.024.

Gao, B., Chen, A., Zhang, W., Li, A., Zhang, C., 2017. Co-production of lipids, eicosapentaenoic acid, fucoxanthin, and chrysolaminarin by Phaeodactylum tricornutum cultured in a flat-plate photobioreactor under varying nitrogen conditions. J. Ocean Univ. Chin. https://doi.org/10.1007/s11802-017-3174-2.

Gao, F., Cabanelas, I.T., Wijffels, R.H., Barbosa, M.J., 2020. Process optimization of fucoxanthin production with Tisochrysis lutea. Bioresour. Technol. 123894. https://doi.org/10.1016/j.biortech.2020.123894.

Garnier, M., Bougaran, G., Pavlovic, M., Berard, J.B., Carrier, G., Charrier, A., Le Grand, F., Lukomska, E., Rouxel, C., Schreiber, N., Cadoret, J.P., Rogniaux, H., Saint-Jean, B., 2016. Use of a lipid rich strain reveals mechanisms of nitrogen limitation and carbon partitioning in the haptophyte Tisochrysis lutea. Algal Res. 20, 229–248. https://doi.org/10.1016/j.algal.2016.10.017.

Grant, C., 2011. Light Intensity Influences on Algal Pigments, Proteins and Carbohydrates: Implications for Pigment-Based Chemotaxonomy. J. Chem. Inf. Model. 53, 1689–1699. https://doi.org/10.1017/CBO9781107415324.004.

Gundermann, K., Büchel, C., 2012. Factors determining the fluorescence yield of fucoxanthin-chlorophyll complexes (FCP) involved in non-photochemical quenching in diatoms. Biochim. Biophys. Acta - Bioenerg. 1817, 1044–1052. https://doi.org/10.1016/j.bbabio.2012.03.008.

Guzmán, H.M., de la Jara Valido, A., Duarte, L.C., Presmanes, K.F., 2010. Estimate by means of flow cytometry of variation in composition of fatty acids from Tetraselmis suecica in response to culture conditions. Aquac. Int. 18, 189–199. https://doi.org/10.1007/s10499-008-9235-1.

Guzmán, H.M., de la Valido, A.J., Duarte, L.C., Presmanes, K.F., 2011. Analysis of interspecific variation in relative fatty acid composition: Use of flow cytometry to estimate unsaturation index and relative polyunsaturated fatty acid content in microalgae. J. Appl. Phycol. 23, 7–15. https://doi.org/10.1007/s10811-010-9526-6.

He, Y., Huang, Z., Zhong, C., Guo, Z., Chen, B., 2019. Pressurized liquid extraction with ethanol as a green and efficient technology to lipid extraction of Isochrysis biomass. Bioresour. Technol. 293, 122049. https://doi.org/10.1016/j.biortech.2019.122049.

Huang, B., Marchand, J., Thiriet-Rupert, S., Carrier, G., Saint-Jean, B., Lukomska, E., Moreau, B., Morant-Manceau, A., Bougaran, G., Mimouni, V., 2019. Betaine lipid and neutral lipid production under nitrogen or phosphorus limitation in the marine microalga Tisochrysis lutea (Haptophyta). Algal Res. 40, 101506. https://doi.org/10.1016/j.algal.2019.101506.

Hyka, P., Lickova, S., Přibyl, P., Melzoch, K., Kovar, K., 2013. Flow cytometry for the development of biotechnological processes with microalgae. Biotechnol. Adv. 31, 2–16. https://doi.org/10.1016/j.biotechadv.2012.04.007.

Katoh, T., Nagashima, U., Mimuro, M., 1991. Fluorescence properties of the allenic carotenoid fucoxanthin: Implication for energy transfer in photosynthetic pigment systems. Photosynth. Res. 27, 221–226. https://doi.org/10.1007/BF00035843.

Kim, S.M., Kang, S.W., Kwon, O.N., Chung, D., Pan, C.H., 2012. Fucoxanthin as a major carotenoid in Isochrysis aff. galbana: Characterization of extraction for commercial application. J. Korean Soc. Appl. Biol. Chem. 55, 477–483. https://doi.org/10.1007/s13765-012-2108-3.

Lee, J.H., Lee, S.H., Yim, S.S., Kang, K.H., Lee, S.Y., Park, S.J., Jeong, K.J., 2013. Quantified high-throughput screening of Escherichia coli producing poly(3-hydroxybutyrate) based on FACS. Appl. Biochem. Biotechnol. 170, 1767–1779. https://doi.

org/10.1007/s12010-013-0311-2.
Li, F.L., Wang, L.J., Fan, Y., Parsons, R.L., Hu, G.R., Zhang, P.Y., 2018. A rapid method for the determination of fucoxanthin in diatom. Mar. Drugs 16, 1–13. https://doi.org/10.3390/md16010033.
Li, M., Wilkins, M., 2020. Flow cytometry for quantitation of polyhydroxybutyrate production by Cupriavidus necator using alkaline pretreated liquor from corn stover. Bioresour. Technol. 295, 122254. https://doi.org/10.1016/j.biortech.2019.122254.
Li, P., Liang, M., Lu, X., Chow, J.J.M., Ramachandra, C.J.A., Ai, Y., 2019. Sheathless Acoustic Fluorescence Activated Cell Sorting (aFACS) with High Cell Viability. Anal. Chem. 91, 15425–15435. https://doi.org/10.1021/acs.analchem.9b03021.
Maeda, H., Fukuda, S., Izumi, H., Saga, N., 2018. Anti-oxidant and fucoxanthin contents of brown alga ishimozuku (Sphaerotrichia divaricata) from the west coast of aomori. Mar. Drugs Jpn. https://doi.org/10.3390/md16080255.
Mairet, F., Bernard, O., Masci, P., Lacour, T., Sciandra, A., 2011. Modelling neutral lipid production by the microalga Isochrysis aff. galbana under nitrogen limitation. Bioresour. Technol. 102, 142–149. https://doi.org/10.1016/j.biortech.2010.06.138.
Miloslavina, Y., Grouneva, I., Lambrev, P.H., Lepetit, B., Goss, R., Wilhelm, C., Holzwarth, A.R., 2009. Ultrafast fluorescence study on the location and mechanism of non-photochemical quenching in diatoms. Biochim. Biophys. Acta - Bioenergy 1787, 1189–1197. https://doi.org/10.1016/j.bbabio.2009.05.012.
Montero, M.F., Aristizábal, M., García Reina, G., 2011. Isolation of high-lipid content strains of the marine microalga Tetraselmis suecica for biodiesel production by flow cytometry and single-cell sorting. J. Appl. Phycol. 23, 1053–1057. https://doi.org/10.1007/s10811-010-9623-6.
Niemi, C., Lage, S., Gentili, F.G., 2019. Comparisons of analysis of fatty acid methyl ester (FAME) of microalgae by chromatographic techniques. Algal Res. 39, 101449. https://doi.org/10.1016/j.algal.2019.101449.
Park, S., Nguyen, T.H.T., Jin, E.S., 2019. Improving lipid production by strain development in microalgae: Strategies, challenges and perspectives. Bioresour. Technol. 292, 121953. https://doi.org/10.1016/j.biortech.2019.121953.
Parkhill, J.P., Maillet, G., Cullen, J.J., 2001. Fluorescence-based maximal quantum yield for PSII as a diagnostic of nutrient stress. J. Phycol. 37, 517–529. https://doi.org/10.1046/j.1529-8817.2001.037004517.x.
Pereira, H., Barreira, L., Mozes, A., Florindo, C., Polo, C., Duarte, C.V., Custádio, L., Varela, J., 2011. Microplate-based high throughput screening procedure for the isolation of lipid-rich marine microalgae. Biotechnol. Biofuels 4, 1–12. https://doi.org/10.1186/1754-6834-4-61.
Pereira, H., Schulze, P.S.C., Schüler, L.M., Santos, T., Barreira, L., Varela, J., 2018. Fluorescence activated cell-sorting principles and applications in microalgal biotechnology. Algal Res. 30, 113–120. https://doi.org/10.1016/j.algal.2017.12.013.
Pyszniak, A.M., Gibbs, S.P., 1992. Immunocytochemical localization of photosystem I and the fucoxanthin-chlorophyll a/c light-harvesting complex in the diatom Phaeodactylum tricornutum. Protoplasma 166, 208–217. https://doi.org/10.1007/BF01322783.
Remmers, I.M., Hidalgo-Ulloa, A., Brandt, B.P., Evers, W.A.C., Wijffels, R.H., Lamers, P.P., 2017. Continuous versus batch production of lipids in the microalgae Acutodesmus obliquus. Bioresour. Technol. 244, 1384–1392. https://doi.org/10.1016/j.biortech.2017.04.093.
Sakurai, T., Aoki, M., Ju, X., Ueda, T., Nakamura, Y., Fujiwara, S., Umemura, T., Tsuzuki, M., Minoda, A., 2016. Profiling of lipid and glycogen accumulations under different growth conditions in the sulfothermophilic red alga Galdieria sulphuraria. Bioresour. Technol. 200, 861–866. https://doi.org/10.1016/j.biortech.2015.11.014.
Swanson, D., Block, R., Mousa, S.A., 2012. Omega-3 Fatty Acids EPA and DHA : Health. J. Adv. Nutr. 3, 1–7. https://doi.org/10.3945/an.111.000893.Omega-3.
Wang, W., Yu, L.J., Xu, C., Tomizaki, T., Zhao, S., Umena, Y., Chen, X., Qin, X., Xin, Y., Suga, M., Han, G., Kuang, T., Shen, J.R., 2019. Structural basis for blue-green light harvesting and energy dissipation in diatoms. Science 80, 363. https://doi.org/10.1126/science.aav0365.
Yen Doan, T.T., Obbard, J.P., 2011. Enhanced lipid production in Nannochloropsis sp. using fluorescence-activated cell sorting. GCB Bioenergy 3, 264–270. https://doi.org/10.1111/j.1757-1707.2010.01076.x.